

clear Physics, Erice, Italy, 1975 (to be published).

²J. P. Boymond *et al.*, Phys. Rev. Lett. **33**, 112 (1974);

J. A. Appel *et al.*, Phys. Rev. Lett. **33**, 719 (1974);

F. W. Büsser *et al.*, Phys. Lett. **53B**, 212 (1974);

D. Bintinger *et al.*, Phys. Rev. Lett. **35**, 72 (1975).

³L. B. Leipuner *et al.*, Phys. Rev. Lett. **36**, 1543 (1975); D. Buchholz *et al.*, Phys. Rev. Lett. **36**, 932 (1976).

⁴L. Baum *et al.*, Phys. Lett. **60B**, 485 (1976).

⁵L. B. Leipuner *et al.*, Phys. Rev. Lett. **34**, 103 (1975).

⁶R. C. Lamb *et al.*, Phys. Rev. Lett. **15**, 800 (1965); R. Burns *et al.*, Phys. Rev. Lett. **15**, 830 (1965); K. Winter, Phys. Lett. **57B**, 479 (1975).

⁷R. Mishke *et al.*, in *Proceedings of the Second Van-derbilt International Conference on New Results in High Energy Physics, Nashville, Tennessee, March 1976* (to be published).

⁸E. W. Beier *et al.*, preceding Letter [Phys. Rev. Lett. **37**, 1114 (1976)].

⁹Portions of our results have been discussed by B. G. Pope, in Proceedings of the European Physical Society International Conference on High Energy Physics, Palermo, Italy, 1975 (unpublished); and by Lederman, Ref. 1. The present Letter extends these preliminary results to lower P_T and to e^- production and includes various refinements in the calculation of expected backgrounds and analysis of the observed signal. The most important improvements were made in the radiative

corrections to electron spectra (which resulted in a reduction of the high P_T signal) and in treatment of η -decay backgrounds.

¹⁰Production rate estimates at 10 and 15 GeV/c include allowances for s dependence and for the beam pion content.

¹¹The fitted π^0/π^- ratios are consistent with $\pi^0 = (\pi^+ + \pi^-)/2$. We neglect direct photons.

¹²For example if the η, ω internal-conversion pair mass distributions did not have a tail extending beyond m_{π^0} , no allowance for η, ω would be necessary.

¹³N. Kroll and W. Wada, Phys. Rev. **98**, 1355 (1955).

¹⁴The γ -ray conversion length as a function of energy and the energy division between e^+ and e^- in pair production, as well as the expression for the bremsstrahlung spectrum, are based on the review by Y. S. Tsai, Rev. Mod. Phys. **45**, 815 (1974).

¹⁵J. B. Marion and B. A. Zimmerman, Nucl. Instrum. Methods **51**, 93 (1967).

¹⁶Because of the nonlinearity in t of the external conversion background, it is difficult to define an accurate extrapolation technique. Therefore, we obtain our results from the data with the bare target, using the calculated background subtractions. We have assigned systematic uncertainties of 50% and 20% to the external and Dalitz conversion background, and 30% to the Compton background.

¹⁷K. Raychaudhuri and H. Weisberg, Phys. Rev. D **13**, 153 (1976).

Experimental Tests of Pomeron Factorization in Single-Particle-Inclusive Hadron Scattering*

E. W. Beier, H. Brody, R. Patton, K. Raychaudhuri, H. Takeda, R. Thern,
R. VanBerg, and H. Weisberg†

Department of Physics, University of Pennsylvania, Philadelphia, Pennsylvania 19174

(Received 19 July 1976)

Measurements of the dependence on $s = (p_a + p_b)^2$ of the cross sections for single charged hadron production in the reactions $a + b \rightarrow c + \text{anything}$ over the range 4 GeV/c $\leq p_a^{\text{lab}} \leq 250$ GeV/c are presented. Particle c is detected in a fixed interval of laboratory momentum and angle in the fragmentation region of the target proton. For the energy range studied there are significant departures from $A + Bs^{-1/2}$ energy dependence. Fits to the s dependence of the cross sections are extrapolated to $s^{-1/2} = 0$ to make seven independent tests of Pomeron factorization.

We report measurements of the cross sections for the single-particle inclusive hadron reactions $a + b \rightarrow c + \text{anything}$ where $a = \pi^+, K^+, p^+$, $b = p$, and $c = \pi^+, K^+, p^+$. The measurements were made in a small, fixed region of the phase space of particle c corresponding approximately to $P_{\perp} = 0.3$ GeV/c and $y_L = 0.6, 0.4,$ and 0.2 for produced $\pi, K,$ and p , respectively.¹ The incident momenta were 4, 6, 8, 10, 12, 15, 20, 24, 150, and 250 GeV/c. The data are interpreted using the Mueller-Regge phenomenology,^{2,3} which suggests that the differential cross sections at high energy should de-

pend on $s = (p_a + p_b)^2$ according to $A + Bs^{-1/2}$. Fits to the s dependence of the measured cross sections are extrapolated to $s^{-1/2} = 0$ and the ratios of the resulting "asymptotic" cross sections are compared with the appropriate total cross-section ratios to test the prediction of Pomeron factorization:

$$\frac{E d^3\sigma/d^3p(ab \rightarrow c)}{E d^3\sigma/d^3p(a'b \rightarrow c)} \stackrel{s \rightarrow \infty}{\approx} \frac{\sigma_{\text{tot}}(ab)}{\sigma_{\text{tot}}(a'b)}, \quad (1)$$

where $\sigma_{\text{tot}}(ab)$ is the total cross section for parti-

cle a scattering on particle b .

Previous studies⁴⁻⁶ of proton fragmentation have utilized bubble chamber data, and have confirmed, in general, the Mueller-Regge phenomenology. These studies, however, often integrate over substantial regions of y_L , p_\perp phase space and often have limited statistical and systematic accuracy. In this Letter, we present results from a systematic study of the dependence of the invariant cross section on s , at fixed y_L and p_\perp using an electronic detector.

The data at $p_a^{\text{lab}} = 150$ and 250 GeV/ c were taken at Fermilab and the data from 4 to 24 GeV/ c were obtained at the Brookhaven National Laboratory alternating gradient synchrotron. For the Fermilab data, two differential Cherenkov counters and one threshold Cherenkov counter provided beam particle identification with negligible contamination of the various particle types. Electron contamination was eliminated by the insertion of 0.4 radiation lengths of lead at the first focus of the beam. Muon contamination is negligible for the high-energy data presented here. The rf bunching of the beam at Fermilab requires that rf buckets populated by more than one particle be rejected. This was achieved by rejecting buckets in which three beam-defining scintillation counters had pulse heights greater than 1.5 times the minimum ionizing pulse height. The measured cross sections are independent of beam intensity at a level of 1% sensitivity, and independent of missteering the beam at the target by ± 0.5 cm in either direction at the level of 3% sensitivity.

The instrumentation of the beam at Brookhaven National Laboratory is fully documented by Beier *et al.*⁷ and will not be discussed here. The same spectrometer was used at both laboratories. The spectrometer is described in detail in Ref. 7, and only a brief summary of its operation is presented here.

The spectrometer is shown schematically in Fig. 1. It is comprised of a small c magnet, eighteen planes of multiwire proportional chambers, three scintillation counters T1-T3 for triggering and particle identification, and a threshold Cherenkov counter C1. Produced protons are separated from faster particles by measuring the time of flight from the target to counter T2. The Cherenkov counter C1 is used to measure the ratio of pions to kaons in the remaining sample of fast particles.

The azimuthal acceptance of the spectrometer, $\Delta\Phi(\theta, p, z)$, is a function of the polar production

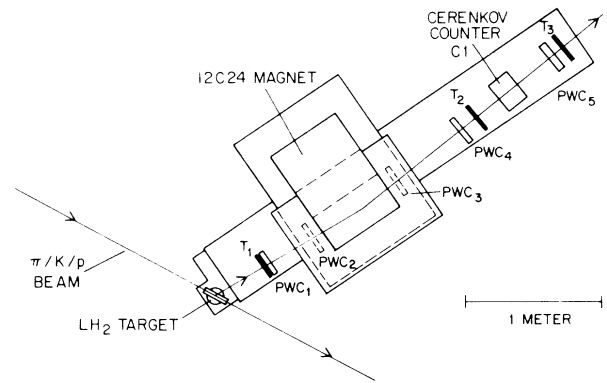


FIG. 1. Plan view of the spectrometer. There are four planes of multiwire proportional chamber in PWC₁₋₄ and two planes in PWC₅.

angle θ , the momentum p , and the longitudinal position in the target z , of the produced particle. The acceptance function integrated over z is used to weight each event within the fiducial volume of the spectrometer. This acceptance correction, as well as energy loss and multiple scattering corrections, are tested by measuring elastic cross sections at low energy where the elastic peak in the distributions of the square of the missing mass is easily resolved. A full discussion of the elastic calibration of the absolute normalization is given in Ref. 7. A further test of the normalization is made by integrating a local fit to the 12 GeV/ c $pp \rightarrow \pi^+$ data of Blobel *et al.*⁸ over the spectrometer acceptance. The results agree with our measurements within 1 standard deviation (about 3%).

The measured cross sections, integrated over the kinematic region specified in Ref. 1, and with empty target backgrounds of typically 3% subtracted, are displayed as a function of $s^{-1/2}$ in Figs. 2(a)-2(d) for produced π^- , π^+ , K^+ , and p , respectively. The production of K^- and p^- in this kinematic range is approximately at the limit of sensitivity of the experiment, and no further conclusions can be made concerning those cross sections.

It is seen from Fig. 2 that the cross section for production of particle c by particle a and its antiparticle \bar{a} approach each other as $s^{-1/2} \rightarrow 0$, in agreement with the prediction of Pomeron factorization.

The pion production cross sections [Figs. 2(a) and 2(b)] are clearly not well described by the parametrization $A + Bs^{-1/2}$ over the large range of s shown. The solid line in these figures represents fits to the expressions $A + Bs^{-1/2} + Cs^{-1}$ for π^+ and

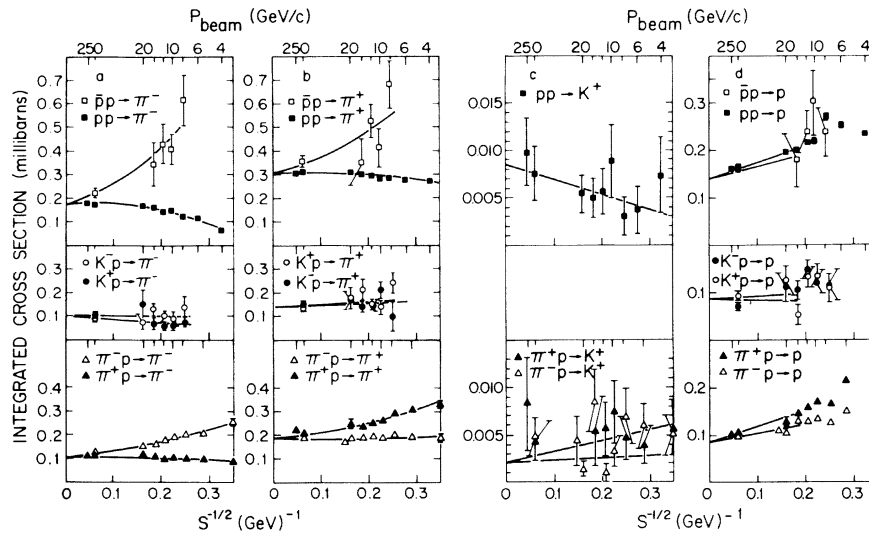


FIG. 2. Cross sections integrated over the kinematic region in Ref. 1, for the production of (a) π^- , (b) π^+ , (c) K^+ , and (d) p . The solid lines are fits to $A + Bs^{-1/2}$ or $A + Bs^{-1/2} + Cs^{-1}$ as described in the text. The tick marks on the abscissa at the top of each part of the figure correspond to the beam momenta at which the cross sections were measured, as described in the text.

p , \bar{p} production of pions, and fits to $A + Bs^{-1/2}$ for the statistically less significant K^+ production of pions. In order to test the hypothesis of Pomeron factorization, the fits are constrained by the requirement that particle and antiparticle production of a given particle be equal at $s^{-1/2} = 0$.

The production of K^+ [Fig. 2(c)] is statistically less significant than π^\pm production, and has been fit to $A + Bs^{-1/2}$. Proton production [Fig. 2(d)] is in the resonance region at low s . A clear signal from the reaction $\pi p \rightarrow A_2 p$ can be seen at $p_a^{\text{lab}} = 6$ GeV/c. Above $p_a^{\text{lab}} = 15$ GeV/c, the proton production has been parametrized by $A + Bs^{-1/2}$.

Extrapolation of the above fits to $s^{-1/2} = 0$ permits asymptotic tests of Pomeron factorization which are independent of assumptions about the low-energy behavior of the cross sections. The ratio of the total cross sections in the limit specified in Eq. (1) is obtained from the parametrization of the diffractive part of the total cross section by Hendrick *et al.*,⁹

$$D_{ap} = C_{ap} \ln[(p_a^{\text{lab}} + m_a)/b_a], \quad (2)$$

evaluated at $p_a^{\text{lab}} = 250$ GeV/c. The resulting tests of Pomeron factorization are presented in Table I. The data allow seven independent tests of Pomeron factorization. Except for K^+ production, where the statistics are poor, the results fall well within the range of the predictions. These results are in agreement with, and extend the result of Ref. 4, which compares two cross sections which were assumed to be independent of s and were integrated from the kinematic limit to $y_{c,\text{M}} = -0.6$.

Further tests of the Mueller-Regge phenomenology, namely relations among the B terms in the above fits, are not possible with the limited high-energy data available at present. We conclude that single-particle inclusive cross sections depart significantly from $A + Bs^{-1/2}$ energy dependence below $p_a^{\text{lab}} \approx 12$ GeV/c at the y and p_\perp measured in this experiment, and thus the range of s over which the Mueller-Regge theory can be applied is established. When these departures are taken into account, extrapolation to $s^{-1/2} = 0$

TABLE I. Tests of Pomeron factorization.

Cross section ratio	Asymptotic ratio of measured cross sections for produced particle type c				Predicted ratio (Ref. 9)
	$c = \pi^-$	$c = \pi^+$	$c = K^+$	$c = p$	
$(\pi p \rightarrow c)/(p p \rightarrow c)$	0.63 ± 0.03	0.62 ± 0.03	0.25 ± 0.18	0.62 ± 0.03	0.61 ± 0.02
$(K p \rightarrow c)/(p p \rightarrow c)$	0.60 ± 0.06	0.45 ± 0.04		0.61 ± 0.08	0.53 ± 0.02

yields asymptotic cross sections which satisfy Pomeron factorization well.

We acknowledge gratefully the assistance of Dr. D. Kreinick, Mr. G. Featherston, Mr. Rolf Brockner, and the staffs of the University of Pennsylvania, Brookhaven National Laboratory, and Fermilab for making this work possible.

*Work performed under the auspices of the U. S. Energy Research and Development Administration.

†Present address: Brookhaven National Laboratory, Upton, N. Y. 11973.

¹The boundaries of the acceptance are $60.75^\circ \leq \theta_c^{\text{lab}} + 3.3^\circ / (p_c^{\text{lab}} - \Delta p_c) \leq 64.25^\circ$ and $0.3 \text{ GeV}/c \leq p_c^{\text{lab}} - \Delta p_c$

$\leq 0.6 \text{ GeV}/c$. Here Δp_c is the momentum lost by particle type c in traversing the apparatus; to sufficient accuracy it is given by $\Delta p_c = (0.0015 \text{ GeV}/c) / \beta_c^3$.

²A. H. Mueller, Phys. Rev. D **2**, 2963 (1970).

³Representative reviews are H. Boggild and T. Ferbel, Annu. Rev. Nucl. Sci. **24**, 451 (1974); R. G. Roberts, in *Phenomenology of Particles at High Energies*, edited by R. L. Crawford and R. Jennings (Academic, London and New York, 1974); and T. Ferbel, SLAC Report No. 179, 1974 (unpublished).

⁴J. Erwin *et al.*, Phys. Rev. Lett. **33**, 1352 (1974).

⁵P. A. Baker *et al.*, Nucl. Phys. **B89**, 189 (1975).

⁶R. Schindler *et al.*, Phys. Rev. Lett. **33**, 862 (1974); J. Whitmore *et al.*, Phys. Lett. **60B**, 211 (1976).

⁷E. W. Beier *et al.*, to be published.

⁸V. Blobel *et al.*, Nucl. Phys. **B69**, 454 (1974).

⁹R. E. Hendrick *et al.*, Phys. Rev. D **11**, 536 (1975).

Blocking Effect in the Transitional Nuclei ^{189,191,193}Au

Y. Gono, R. M. Lieder, M. Müller-Veggian, A. Neskakis, and C. Mayer-Böricke
Institut für Kernphysik der Kernforschungsanlage Jülich, D-517 Jülich, West Germany

(Received 26 July 1976)

The study of high-spin states in ^{189,191,193}Au revealed that the $h_{11/2}$ proton-hole rotation-aligned bands are terminated by isomeric $\frac{27}{2}^-$ states most probably of $(\pi h_{11/2}^{-3})_{27/2}^-$ configuration. The relatively low excitation energies of these isomers can be understood qualitatively if the concept of blocking as used in the rotation-alignment model is modified by taking into account a reduction of the proton pairing gap energy in these odd-mass Au nuclei.

Recent in-beam γ -spectroscopy and radioactive decay studies of the odd-mass Au isotopes ¹⁸⁷⁻¹⁹⁵Au¹⁻⁶ revealed many interesting features. A remarkable result of these studies is the existence of bands originating from the $h_{11/2}$ proton-hole state in ^{187,189,191,193,195}Au (Refs. 1-6) as well as from the $h_{9/2}$ proton state in ^{187,189,191}Au (Refs. 2-4). The bands originating from the $h_{11/2}$ proton-hole state in ^{191,193,195}Au have been interpreted by Tjóm *et al.*¹ as rotation-aligned bands within the framework of the rotation-alignment (RAL) model⁷ in which the odd nucleon is coupled to a symmetric rotating core. Calculations⁸ using an axially asymmetric rotating core yielded a better agreement with the experimental results for these bands. The $h_{11/2}$ and $h_{9/2}$ bands observed in ^{187,189}Au (Refs. 2 and 3) have been similarly interpreted. In order to understand the existence of the $h_{9/2}$ and $h_{11/2}$ rotation-aligned bands in these Au nuclei, it has been assumed, in the framework of the RAL model, that they have a prolate shape in the $h_{9/2}$ state and an oblate shape in the $h_{11/2}$ state.² From calculations⁹ in the framework of the triaxial-rotor-plus-particle model, this shape coexistence was attributed to different

asymmetry parameters γ . In case of ¹⁸⁹Au, $\gamma = (37 \pm 2)^\circ$ for the $h_{11/2}$ band and $\gamma = (23 \pm 2)^\circ$ for the $h_{9/2}$ band.⁹ These values are essentially the asymmetry parameters of ¹⁹⁰Hg and ¹⁸⁸Pt which are considered as the core nuclei of ¹⁸⁹Au in the two respective states.⁹

Although the low spin states of the $h_{11/2}$ bands in ^{193,195}Au can be well understood also in the framework of the particle-vibration coupling model,¹⁰ the RAL model has been applied more commonly to explain high-spin yrast states. Therefore, this latter model has been applied in the present work to interpret the bands observed in ^{189,191,193}Au.

Prior to our study, the $h_{11/2}$ proton-hole rotation-aligned bands were definitely established up to $\frac{23}{2}^-$ in ^{187,189,191,193}Au (Refs. 1-3) and up to $\frac{19}{2}^-$ in ¹⁹⁵Au (Ref. 1). It was the aim of the present study to reinvestigate ^{189,191,193}Au in order to extend the $h_{11/2}$ bands to higher spin states for the following reason. In the Hg core nuclei ^{190,192,194}Hg 10⁺ isomers have been observed¹¹ which are considered to have a $(\pi h_{11/2}^{-2})_{10+}$ two-proton-hole configuration. The upper portion of the ground-state bands (gsb) in ^{192,194}Hg (Ref. 11) built on top